



Original Article



# Mitochondrial reactive oxygen species promote mitochondrial damage in high glucose-induced dysfunction and apoptosis of human dental pulp cells

Shuo Tao <sup>a,b</sup>, Ting Yang <sup>a,b</sup>, Yue Yin <sup>a,b</sup>, Qi Zhang <sup>a,b\*</sup>

<sup>a</sup> Department of Endodontics, Stomatological Hospital and Dental School of Tongji University, Shanghai, China

<sup>b</sup> Shanghai Engineering Research Centre of Tooth Restoration and Regeneration, Shanghai, China

Received 27 March 2023; Final revision received 10 April 2023

Available online 21 April 2023

## KEYWORDS

Diabetes;  
High glucose;  
Dental pulp cell;  
Mitochondrial  
reactive oxygen  
species;  
Mitochondrial  
dysfunction

**Abstract** *Background/purpose:* High glucose (HG)-induced aberrant proliferation, apoptosis and odontoblastic differentiation of dental pulp cells (DPCs) have been implicated in the pathogenesis of impaired diabetic pulp healing; however, the underlying mechanism remains unclear. This study aimed to investigate the role of mitochondrial reactive oxygen species (mtROS) and mitochondria in HG-induced dysfunction and apoptosis of DPCs.

*Materials and methods:* Human DPCs (hDPCs) were cultured in a low-glucose, high-glucose, mannitol, and MitoTEMPO medium in vitro. Methylthiazol tetrazolium assay, Annexin V-FITC/PI staining and scratch-wound assay were used to analyze cell proliferation, apoptosis and migration, respectively. Alkaline phosphatase staining and alizarin red S staining were used to evaluate cell differentiation. DCF-DA staining, MitoSOX staining, MitoTracker Red staining, JC-1 staining, and adenosine triphosphate (ATP) kit assay were performed to investigate total ROS and mtROS generation, mitochondrial density, mitochondrial membrane potential (MMP), and ATP synthesis, respectively. Quantitative PCR assay was performed to detect the mRNA expression of mitochondrial biogenesis- and dynamics-related markers. Transmission electron microscopy was used to observe the mitochondrial ultrastructure.

*Results:* HG augmented the production of total ROS and mtROS, and triggered mitochondrial damage in hDPCs, as reflected by decreased mitochondrial density, depolarized MMP, reduced ATP synthesis, altered mRNA expression of mitochondrial biogenesis- and dynamics-related markers, and abnormal mitochondrial ultrastructure. Supplementation of MitoTEMPO alleviated the mitochondrial damage and reversed the aberrant proliferation, apoptosis, migration and odontoblastic differentiation of HG-stimulated hDPCs.

\* Corresponding author. Department of Endodontics, Stomatological Hospital and Dental School of Tongji University, Shanghai Engineering Research Centre of Tooth Restoration and Regeneration, 399 Middle Yanchang Road, Shanghai, 200072, China.

E-mail address: [qizhang@tongji.edu.cn](mailto:qizhang@tongji.edu.cn) (Q. Zhang).

**Conclusion:** HG triggers mitochondrial damage via augmenting mtROS generation, resulting in the inhibited proliferation, migration, and odontoblastic differentiation of hDPCs and enhanced their apoptosis.

© 2023 Association for Dental Sciences of the Republic of China. Publishing services by Elsevier B.V. This is an open access article under the CC BY-NC-ND license (<http://creativecommons.org/licenses/by-nc-nd/4.0/>).

## Introduction

Diabetes mellitus (DM) is a group of metabolic disorders characterized by hyperglycemia and is one of the most common systemic diseases worldwide.<sup>1</sup> The International Diabetes Federation has estimated 693 million people to suffer from by 2045.<sup>1</sup> In people with DM, a high level of blood glucose causes structural changes and impairment in self-repair ability in various tissues, resulting in the development of disability-causing and life-threatening medical complications, such as diabetic nephropathy, diabetic foot ulcer, and diabetic cardiovascular diseases.<sup>2</sup> With the rapid increase in DM incidence, endodontic research on DM-associated pathologic modifications at the dental pulp level is emerging.<sup>3–5</sup> Constricted pulp cavity and modifications in pulp components have been observed in diabetic pulp tissues.<sup>3,4</sup> Additionally, impaired reparative dentin formation and poor wound healing have been reported after direct pulp capping procedures in streptozotocin-induced diabetic rats.<sup>5</sup> A few in vitro studies have shown that dental pulp cells (DPCs) manifest aberrant proliferation, apoptosis, and odontoblastic differentiation in a high-glucose environment.<sup>6,7</sup> These findings suggest that impairment in dentin bridge formation in diabetic pulp tissues could be attributable to the dysfunction and apoptosis of DPCs under high-glucose conditions; however, the possible underlying mechanism remains unclear.

Available evidence has shown that the overproduction of hyperglycemia-induced mitochondrial reactive oxygen species (mtROS) is a unifying mechanism that regulates abnormal cellular events through four major biochemical pathways, namely, polyol pathway, advanced glycation end products, protein kinase C isoforms, and hexosamine pathway, in various diabetic tissues.<sup>8,9</sup> Even though the mitochondrial hormesis theory challenged this view, mtROS remains the key regulator of the development of diabetic complications.<sup>10</sup> Mitochondria are the major source of mtROS and also the principal target of mtROS.<sup>11</sup> Excessive production of mtROS directly causes oxidative damage to mitochondrial proteins and affects mitochondrial membrane potential (MMP), adenosine triphosphate (ATP) production, mitochondrial biogenesis, and mitochondrial dynamics.<sup>12</sup> Mitochondrial damage caused by mtROS further amplify the initial oxidative stress through the so-called ROS-induced ROS release, wherein they aggravate each other and result in cell dysfunction and apoptosis.<sup>13</sup> mtROS and mitochondria have recently been regarded as critical modulators in endothelial cells, osteoblasts, and periodontal ligament cells, and any disturbance in mitochondrial homeostasis caused by mtROS leads to endothelial injury, abnormalities in bone metabolism, and aggravated periodontitis in diabetic conditions.<sup>14–16</sup>

However, the role of mtROS and mitochondria in high glucose-induced DPC injuries remains unreported.

Therefore, this study aimed to investigate the role of mtROS-mediated mitochondrial damage in the dysfunction and apoptosis of DPCs under high-glucose conditions to provide a theoretical basis and unravel potential therapeutic targets for the treatment of impaired pulp healing in DM individuals.

## Materials and methods

### Cell isolation and culture

The procedure used for extracting human healthy dental pulp was approved by the Institutional Review Board of Tongji University (SL2018R5). After obtaining informed consent, human DPCs (hDPCs) were harvested from healthy permanent third molars of patients aged 18–25 years at Affiliated Stomatology Hospital of Tongji University. The hDPCs were cultured in 5.5 mM D-glucose Dulbecco's Modified Eagle Medium (DMEM; Gibco, Grand Island, NY, USA) containing 10% fetal bovine serum (FBS; Gibco), 100 U/mL penicillin (Gibco), and 100 mg/mL streptomycin (Gibco). The cells were divided into the control group (DMEM containing 5.5 mM glucose), high-glucose (HG) group (DMEM containing 30 mM glucose; Sangon Biotech, Shanghai, China), mannitol (Man) group (osmotic control group; DMEM containing 5.5 mM glucose and 24.5 mM Man; Sangon Biotech), and MitoTEMPO (MT) group (DMEM containing 30 mM glucose and 1 mM MT; Sigma-Aldrich, St. Louis, MO, USA).

### Cell proliferation assay

The proliferation of hDPCs was assessed using methylthiazol tetrazolium (MTT) assay on days 1, 3, 5, and 7 according to the manufacturer's protocols. Briefly, the hDPCs were cocultured with MTT (Thermo Fisher Scientific, Waltham, MA, USA) at 37 °C for 4 h. Then MTT was reduced to formazan crystals by adding dimethylsulfoxide (Thermo Fisher Scientific). The absorbance was measured at 570 nm using a microplate reader (Bio-Tek, Winooski, VT, USA).

### Annexin V-FITC/PI staining

Cellular apoptosis was determined using the Annexin V-FITC/PI double staining, and the cells were counted using a flow cytometer (Beckman Coulter, Pasadena, CA, USA) as previously reported.<sup>17</sup> The dots in the upper left quadrant, lower left quadrant, upper right quadrant, and lower right quadrant indicate damaged cells (Annexin V-, PI+), viable

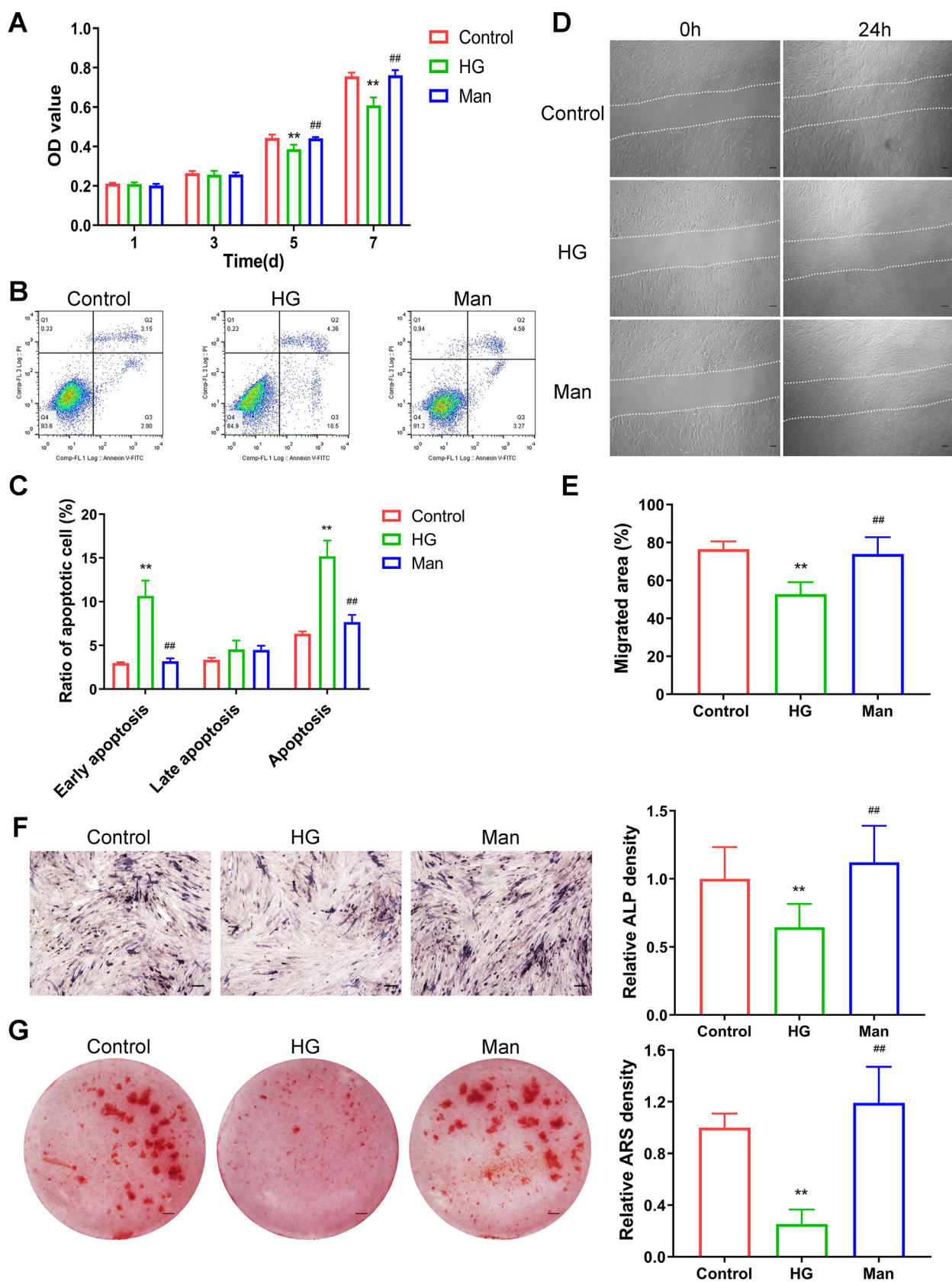


**Figure 1** Abnormal biological behaviors of hDPCs under high-glucose conditions. (A) Cell proliferation was measured by MTT assay at 1, 3, 5 and 7 days. (B) Cell apoptosis was detected by Annexin V-FITC/PI staining. (C) The quantification analysis of the ratio of apoptotic cells. (D) Cell migration was detected by scratch-wound assay at 0 and 24 h. The dot lines indicate the total area of the wound site. Scar bar: 50  $\mu$ m. (E) The percentage of migrated area at 24 h after scratching the cells. (F) Cell differentiation was

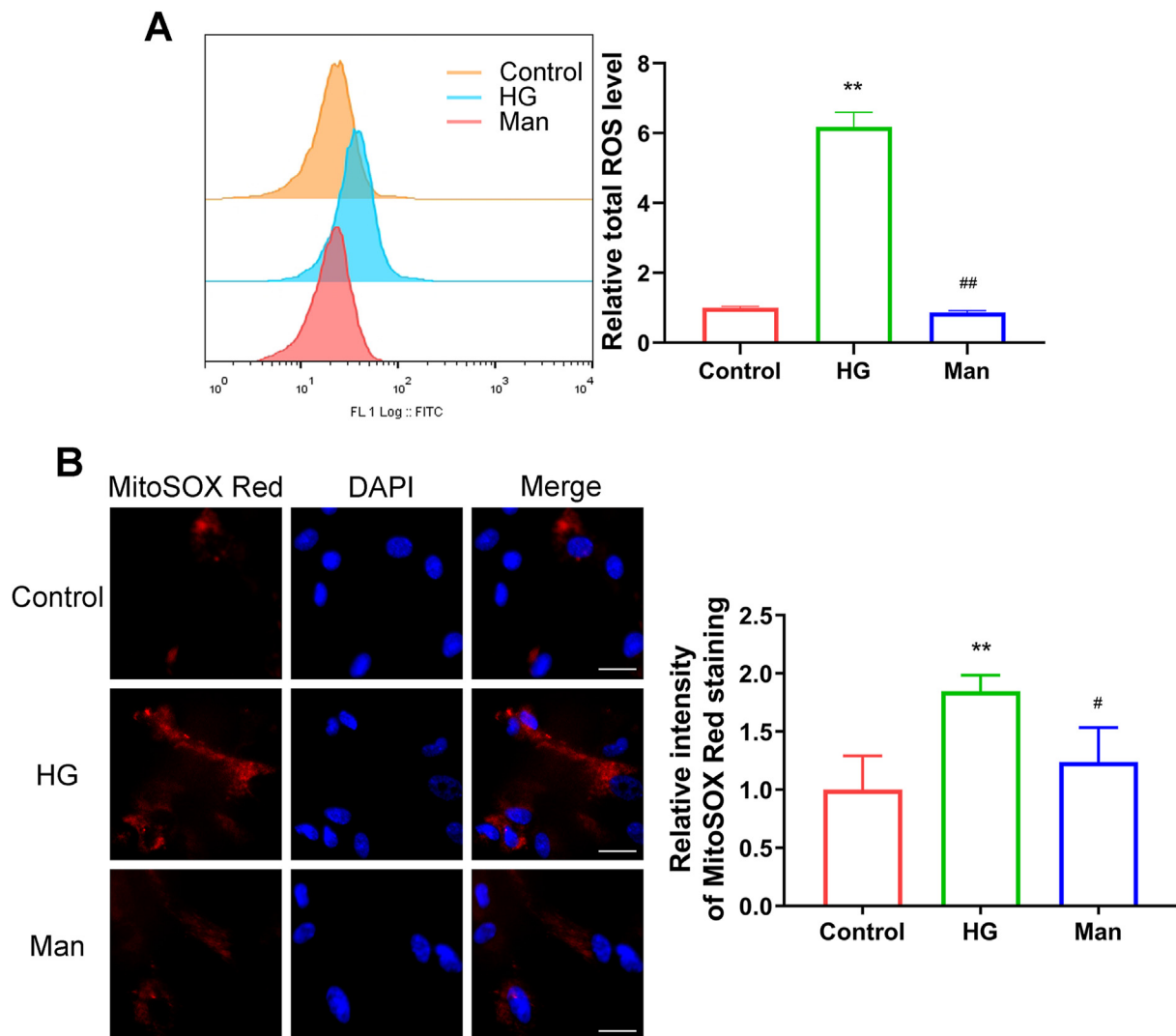


**Figure 2** Excessive ROS and mtROS generation in hDPCs under high-glucose conditions. (A) The level of total ROS was evaluated with the intensity of DCF-DA fluorescence. Right panel shows the quantification of the DCF-DA fluorescence intensity using flow cytometry. (B) The mtROS generation was measured by the MitoSOX Red fluorescence. Scale bar: 25 μm. Right panel shows the quantification of the fluorescence intensity of MitoSOX Red. Data are presented as the mean ± SD of three independent experiments. \*\*P < 0.01 compared to the control group. #P < 0.05, ##P < 0.01 compared to the HG group.

cells (Annexin V-, PI-), cells in late apoptosis (Annexin V+, PI+), and cells in early apoptosis (Annexin V+, PI-), respectively.

#### Scratch-wound assay

Cell migration was analyzed using scratch-wound assay as described previously.<sup>18</sup> Briefly, a 1000-mL rile pipette tip was used to scratch a confluence cell monolayer to obtain a “wound line.” Images of the wounds were captured at 0 and 24 h under an inverted microscope (Carl Zeiss, Jena,

Germany). The migrated area was analyzed using ImageJ software (National Institute of Health, Bethesda, MD, USA).

#### Alkaline phosphatase staining and alizarin red S staining

To induce odontoblastic differentiation, hDPCs were cultured in the odontoblastic medium (OM) containing 50 mg/mL ascorbic acid (Sigma-Aldrich), 10 mmol/L β-glycerophosphate (Sigma-Aldrich), and 100 nmol/L dexamethasone (Sigma-Aldrich) for 14 and 21 days. After

assessed by intracellular ALP staining. Scale bar: 200 μm. Right panel shows the quantification of ALP staining density. (G) Cell differentiation was evaluated by ARS staining. Scale bar: 5 mm. Right panel shows the quantification of ARS staining density. Data are presented as the mean ± SD of three independent experiments. \*\*P < 0.01 compared to the control group. ##P < 0.01 compared to the HG group.

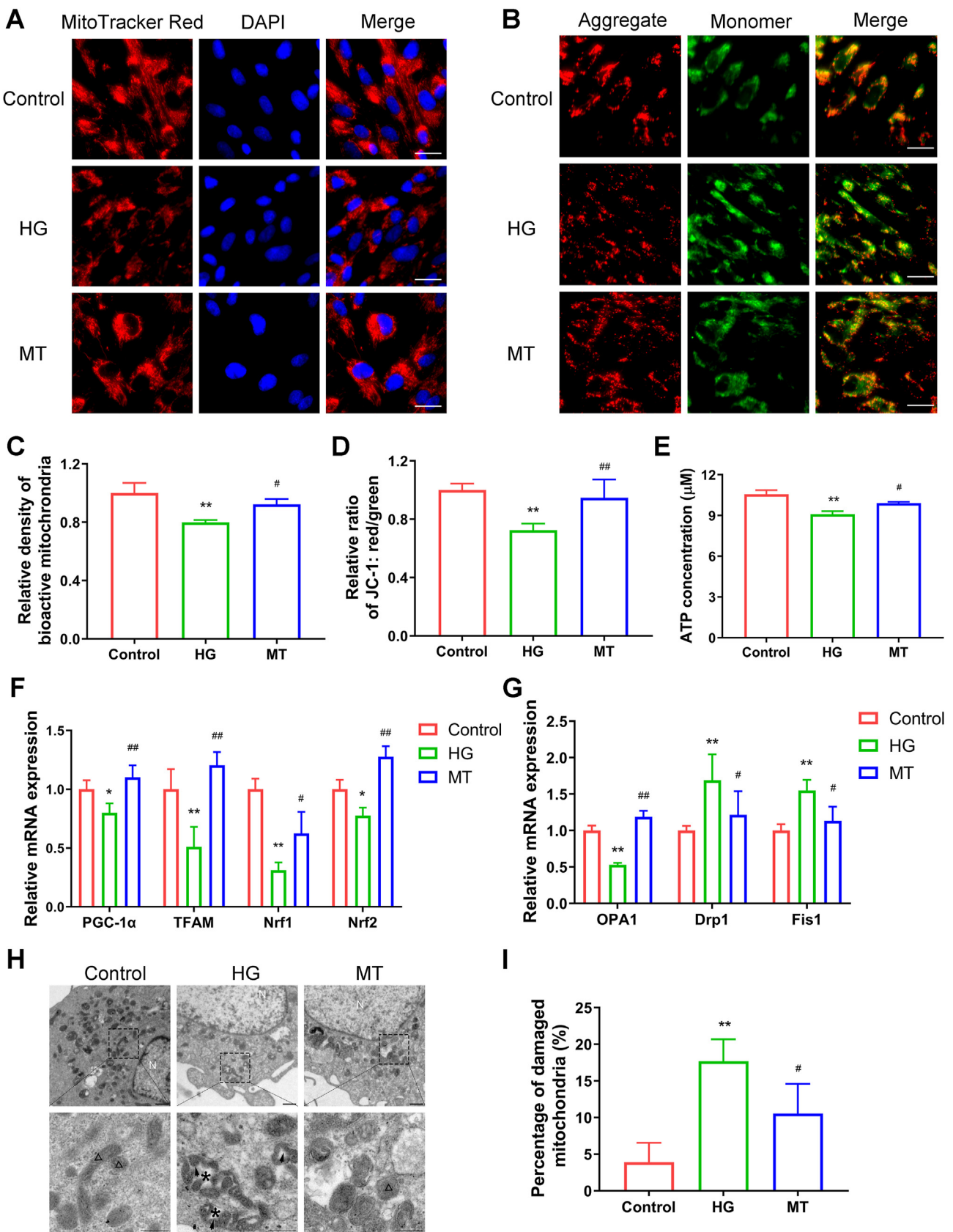


**Figure 3** High glucose triggered the mitochondrial damage by augmenting mtROS generation in hDPCs. (A) The density of bioactive mitochondria was assessed by MitoTracker Red staining. Scar bar: 25  $\mu$ m. (B) The mitochondrial membrane potential (MMP) was evaluated by JC-1 staining. Scar bar: 25  $\mu$ m. (C) The quantitation of bioactive mitochondrial density. (D) The

incubation, cells were subjected to alkaline phosphatase (ALP) staining (Beyotime, Shanghai, China) and alizarin red S (ARS) staining (Sigma-Aldrich) according to manufacturer's instructions, respectively. The ALP-positive areas were analyzed under a phase-contrast microscope (Nikon Eclipse 80i, Tokyo, Japan), and the ARS-positive areas were analyzed under a stereoscopic microscope (Carl Zeiss). The staining density was measured using ImageJ software (National Institute of Health).

### Evaluation of intracellular total ROS and mtROS generation

The hDPCs were incubated with 2',7'-dichlorofluorescein diacetate (DCF-DA, Sigma-Aldrich) fluorescent dye to evaluate the intracellular total ROS level. The relative level of fluorescence was quantified using flow cytometry (Beckman Coulter). Additionally, the hDPCs were incubated with the fluorescent probe MitoSOX Red (Invitrogen, Carlsbad, CA, USA) to measure the mtROS level. The nuclei were stained with Hoechst 33342 (Beyotime). MitoSOX Red fluorescence was determined under a fluorescence microscope (Carl Zeiss).

### MitoTracker red staining

To determine the bioactive mitochondrial density, hDPCs were incubated with the fluorescent probe MitoTracker Red CMXRos (Invitrogen). The fluorescence was detected and quantified under a fluorescence microscope.

### Intracellular MMP analysis

The MMP was estimated using the JC-1 staining (Beyotime) according to manufacturer's instructions. The hDPCs were incubated with the JC-1 dye at 37 °C. The red and green fluorescence of the JC-1 dye was investigated under a fluorescence microscope. Mitochondrial depolarization is indicated by a decrease in the red/green fluorescence ratio. Thus, the data for quantitative analysis was presented as the mean value of the red/green fluorescence ratio.

### Intracellular ATP detection

Intracellular ATP levels were detected using an ATP detection kit (Beyotime) according to manufacturer's protocols. The hDPCs were homogenized and sonicated in a lysis buffer. Supernatants were obtained after centrifugation at 4 °C. The ATP content was quantified using a luminescence plate reader (Bio-Tek).

quantitation of JC-1 red/green ratio. (E) The ATP synthesis was detected in hDPCs. (F) The mitochondrial biogenesis-related genes expression of *PGC-1α*, *TFAM*, *Nfr1* and *Nrf2* were measured by qPCR analysis. (G) The mitochondrial dynamics-related genes expression of *OPA1*, *Drp1* and *Fis1* were measured by qPCR analysis. (H) The mitochondrial ultrastructure was observed using TEM analysis. The lower panel is the higher magnification view of the boxed region in the upper panel. Triangles indicate the healthy mitochondria. Asterisks indicate the damaged mitochondria. Arrows indicate mitochondrial cristae disarrangement and ablation. Scar bar: 10 μm in the upper panel and 5 μm in the power panel. (I) The quantification of the percentage of damaged mitochondria in hDPCs. Data are presented as the mean ± SD of three independent experiments. \*P < 0.05, \*\*P < 0.01 compared to the control group. #P < 0.05, ##P < 0.01 compared to the HG group.

### Quantitative real-time polymerase chain reaction

Quantitative real-time polymerase chain reaction (qPCR) analysis was performed to determine the mRNA expression of mitochondrial biogenesis- and dynamics-related markers. The hDPCs were homogenized with Trizol reagent (Invitrogen), and 1 mg of isolated mRNA was reverse-transcribed with M-MLV Reverse Transcriptase (Promega, Madison, WI, USA) according to manufacturer's instructions. The primers used are listed in Appendix Table 1. The human *β-actin* gene was used as an endogenous control for each sample.

### Transmission electron microscopy

The ultrastructure and mass of the mitochondria in hDPCs were examined using transmission electron microscopy (TEM). The hDPCs were fixed with 2.5% glutaraldehyde, post-fixed with 1% OsO<sub>4</sub>, dehydrated with standard ethanol series, embedded in epoxy resin, and then cut into 60-nm-thick slides. After heavy metal staining with 2% uranium acetate and 2.6% lead citrate, the slides were examined using a transmission electron microscope (Hitachi, Tokyo, Japan). The percentage of damaged mitochondria was evaluated from three cells in three different visual fields on one specimen, with three specimens in each group.

### Statistical analysis

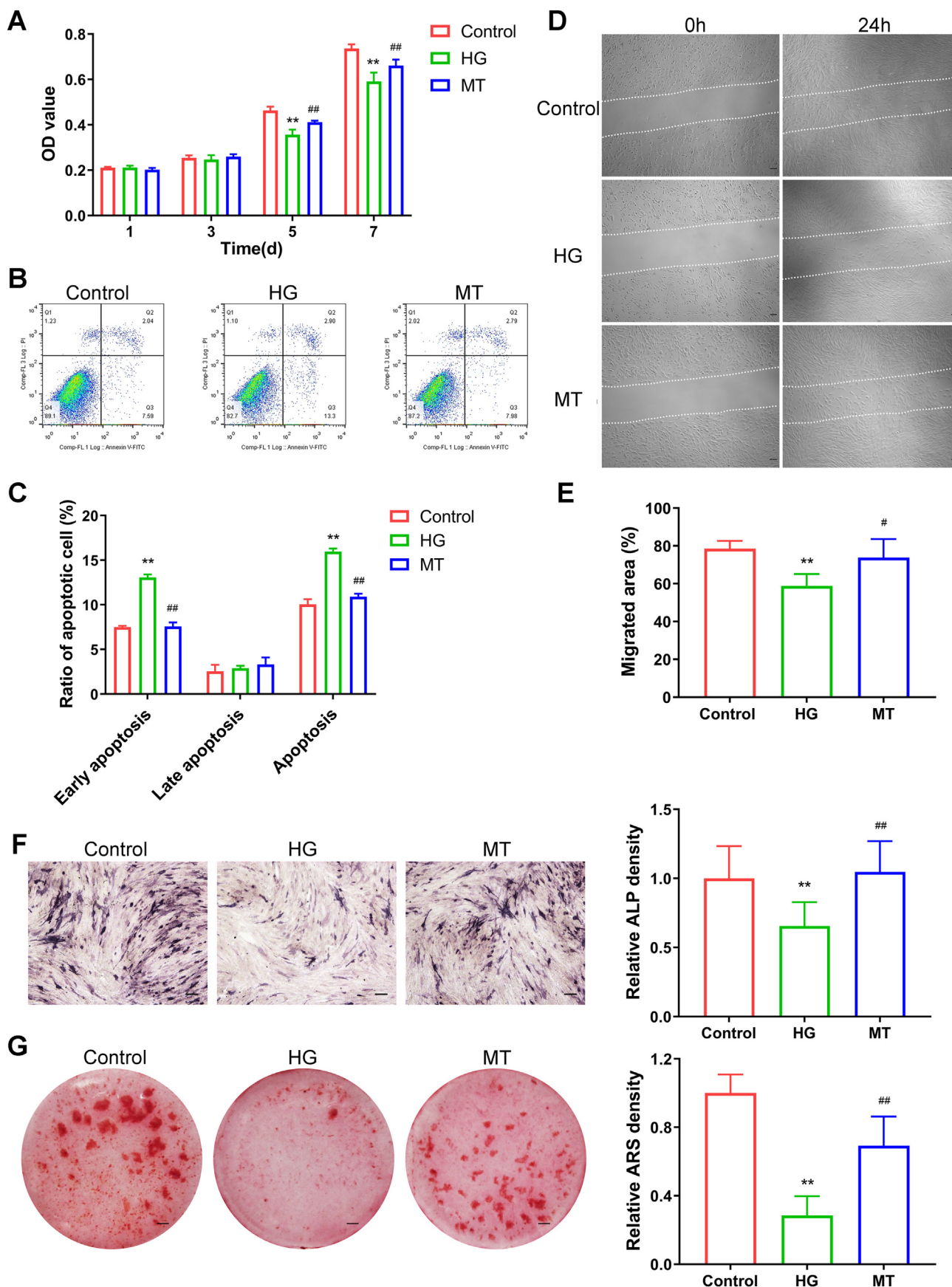
Experiment data were statistically tested by SPSS 21.0 and GraphPad Prism 9.0. The results are presented as mean ± SD of three independent biological experiments. Statistical comparisons among groups were conducted using one-way or two-way ANOVA when applicable. The difference was considered statistically significant at P < 0.05 level.

## Results

### Abnormal biological behaviors of hDPCs under high-glucose conditions

Cell proliferation was assessed using the MTT assay. As shown in Fig. 1A, HG treatment significantly inhibited cell proliferation on days 5 and 7 compared with the control group, but no significant difference in cell proliferation existed between the control and Man groups.

To analyze the apoptotic cell proportion, the Annexin V-FITC/PI double-staining was performed. As shown in Fig. 1B and C, the total apoptotic rate in the HG group was significantly higher than that in the control and Man groups



on day 7. The early apoptotic cell rate was higher in the HG group than that in the control and Man groups, whereas no significant difference in the late apoptotic cell rate existed between the control and HG groups.

To detect the cell migration, the scratch-wound assay was performed. Compared with the control and Man groups, HG treatment significantly decreased the percentage of cell migration area at 24 h after scratching the cells (Fig. 1D and E).

To evaluate the cell odontoblastic differentiation, the ALP staining and ARS staining were performed on days 14 and 21, respectively. As shown in Fig. 1F and G, the density of ALP staining and ARS staining were significantly decreased by HG treatment.

### Excessive ROS and mtROS generation in hDPCs under high-glucose conditions

The intracellular total ROS level was determined based on the intensity of the DCF-DA fluorescence after 7 days of incubation. As shown in Fig. 2A, compared with the control group, the HG group showed a significant increase in fluorescence intensity. The mtROS levels were then evaluated by incubating hDPCs with the fluorophore MitoSOX Red, a dye that selectively targets mitochondria. As shown in Fig. 2B, HG-treated hDPCs showed a significant increase in fluorescence intensity compared with the control group.

### High glucose triggered the mitochondrial damage by augmenting mtROS generation in hDPCs

To investigate the role of mtROS and mitochondrial damage in the dysfunction and apoptosis of hDPCs under high-glucose conditions, the recovery effect of MT on HG-stimulated hDPC injuries was assessed after 7 days of incubation; MT is a mitochondria-targeted ROS scavenger and exerts a protective effect on the mitochondria.<sup>19</sup> As shown in Figs. S1A and B, additional treatment with MT eliminated total ROS and mtROS generation in HG-stimulated hDPCs. As shown in Fig. 3A and C, the bioactive mitochondrial density in the HG group were significantly lower than that in the control group. However, MT treatment significantly increased the mitochondrial density under high-glucose conditions. To evaluate the mitochondrial function, MMP and ATP production were measured. As shown in Fig. 3B and D, the JC-1 red/green fluorescence ratio significant decreased after exposure to high glucose, indicating the MMP depolarization. However, MT administration reversed the HG-induced drop of MMP. A significant reduction in ATP production was observed in the HG group compared with

that in the control group, but MT administration attenuated HG-suppressed ATP production (Fig. 3E).

Mitochondria are dynamic organelles that continuously undergo movement, fusion and division. Normal mitochondrial function is maintained through tightly regulated mechanisms involving biogenesis, fusion and fission.<sup>20</sup> We then investigated whether there were alterations in mitochondrial biogenesis and fusion-fission dynamics in hDPCs under high-glucose conditions. As shown in Fig. 3F, the mRNA expression of mitochondrial biogenesis-related factors, namely, *PGC-1 $\alpha$* , *TFAM*, *Nrf1*, and *Nrf2*, were downregulated in the HG group compared with that in the control group. HG treatment also led to a decline in the mRNA expression of the pro-fusion factor *OPA1* and an increase in the mRNA expression of the pro-fission factors *Drp1* and *Fis1* (Fig. 3G). As for the pro-fusion factors *Mfn1* and *Mfn2*, the HG group showed similar mRNA expression as that of the control group (Fig. S2). Following MT treatment, the mRNA expression of *PGC-1 $\alpha$* , *TFAM*, *Nrf1*, *Nrf2*, and *OPA1* were upregulated, and the mRNA expression of *Drp1* and *Fis1* were downregulated in HG-cultured hDPCs (Fig. 3F and G).

The mitochondrial ultrastructure was further assessed by TEM analysis. As shown in Fig. 3H, mitochondria in hDPCs demonstrated indications of damage, including a swollen appearance, cristae disarrangement and ablation, as well as reduced electron density of the mitochondrial matrix under high-glucose conditions. The statistical data revealed that HG treatment amplified the percentage of damaged mitochondria when compared with that in the control group; however, MT administration recovered the HG-induced damage to the mitochondrial ultrastructure in hDPCs (Fig. 3I).

### MT attenuated the dysfunction and apoptosis of hDPCs under high-glucose conditions

Additional treatment with MT recovered the abnormal biological behaviors of hDPCs under high-glucose conditions. As shown in Fig. 4A, MT promoted the cell proliferation in HG-stimulated hDPCs. Decreased apoptosis (Fig. 4B and C) and increased migration (Fig. 4D and E) were also observed in hDPCs following MT treatment under high-glucose conditions. Moreover, MT administration ameliorated the HG-suppressed odontoblastic differentiation of hDPCs in the high-glucose environment (Fig. 4F and G).

## Discussion

DM is a metabolic disease associated with dysfunction of various tissues due to the high level of blood glucose.<sup>1</sup> Owing to the rapid increase in the DM patient population,

**Figure 4** MT attenuated the dysfunction and apoptosis of hDPCs under high-glucose conditions. (A) Cell proliferation was measured by MTT assay at 1, 3, 5 and 7 days. (B) Cell apoptosis was detected by Annexin V-FITC/PI staining. (C) The quantification analysis of the ratio of apoptotic cells. (D) Cell migration was detected by scratch-wound assay at 0 and 24 h. The dot lines indicate the total area of the wound site. Scar bar: 50  $\mu$ m. (E) The percentage of migrated area at 24 h after scratching the cells. (F) Cell differentiation was assessed by intracellular ALP staining. Scar bar: 200  $\mu$ m. Right panel shows the quantification of ALP staining density. (G) Cell differentiation was evaluated by ARS staining. Scar bar: 5 mm. Right panel shows the quantification of ARS staining density. Data are presented as the mean  $\pm$  SD of three independent experiments. \*\* $P$  < 0.01 compared to the control group.  $^{\#}P$  < 0.05,  $^{##}P$  < 0.01 compared to the HG group.

emerging research suggests that dental pulp tissue could be affected by DM.<sup>3–5</sup> Deficient wound healing can occur after direct pulp capping procedures in DM rats.<sup>5</sup> A few in vitro studies have shown that high glucose suppresses proliferation and odontoblastic differentiation and enhances apoptosis of DPCs, which may be a possible explanation for the impaired diabetic pulp healing.<sup>6,7</sup> However, the molecular mechanism underlying this phenomenon has not been reported yet. Compromised wound healing in DM involves a complex pleiotropic etiology, and the present research pointed out the major events of wound healing as a target of excessive mtROS generation according to the mitochondrial superoxide theory proposed by Brownlee.<sup>21</sup> In recent years, mitochondrial dysfunction mediated by mtROS overproduction has been regarded to have another, but no less important, role in DM-induced oxidative stress injuries and diabetic complications.<sup>22</sup> Hu et al.<sup>16</sup> suggested that mitochondria are a key regulator of proliferation, differentiation, and survival of osteoblasts that directly affect the osteointegration of the titanium implant. Sun et al.<sup>15</sup> proposed that mitochondrial dysfunction aggravates periodontitis in DM rats. In this study, we for the first time present in vitro evidence that mitochondrial damage mediated by mtROS can contribute to HG-induced dysfunction and apoptosis of hDPCs. Previously, only a few in vitro studies have clarified the role of mitochondrial dysfunction in DPC death induced by lipopolysaccharide or oxidative stress.<sup>23–25</sup> Our findings may therefore provide important clues regarding the pathogenesis of impaired pulp healing in other pathological conditions including DM.

In accordance with previous reports,<sup>6,7</sup> HG treatment significantly inhibited the proliferation and odontoblastic differentiation and activated the apoptosis of hDPCs in vitro in this study. Moreover, the migration of hDPCs declined under high-glucose conditions, consistent with the result of decreased migration of human dental pulp stem cells (hDPSCs) derived from DM patients as reported by Emel et al.<sup>26</sup> Decreased proliferation and odontoblastic differentiation of hDPSCs derived from DM patients were also reported by Emel et al.<sup>26</sup> However, a previous report showed that the proliferation and osteogenic differentiation of hDPSCs were not affected by high glucose (20 mM) environment.<sup>27</sup> This might be due to different concentrations of glucose in the culture medium, since another report showed that high glucose (25 mM) content could affect the proliferation and differentiation potential of hDPCs<sup>28</sup> and the glucose concentration in HG group was 30 mM in our study. In line with such abnormalities in biological behaviors, mtROS generation significantly increased as observed on direct mitochondrial superoxide staining in hDPCs under high-glucose conditions. Previous studies have revealed that mtROS overproduction could impair cellular function and activate apoptosis, resulting in deficient wound healing of tissues in DM.<sup>29</sup> Mitochondria-targeted antioxidants such as MT are effective in eliminating mtROS and ameliorating oxidative stress-related diseases.<sup>19</sup> Thus, in the present study, MT treatment was applied to verify the role of mtROS in HG-induced hDPC injuries. The results of the recovery effect of MT demonstrated that mtROS suppressed the proliferation, migration, and

odontoblastic differentiation of hDPCs and enhanced their apoptosis in the high-glucose environment.

Accumulating evidence has shown that mtROS induces mitochondrial damage, which play an important role in the pathogenesis of diabetic complications.<sup>22</sup> In this study, our findings revealed that HG treatment reduced the density of bioactive mitochondria, damaged the mitochondrial ultra-structure, depolarized MMP, diminished ATP production, compromised mitochondrial biogenesis, and induced imbalance in mitochondrial dynamics in hDPCs in vitro. Moreover, these abnormal mitochondrial events were regulated by mtROS and were closely associated with HG-induced dysfunction and apoptosis of hDPCs. Enzymes of the electronic transport chain (ETC), especially complex I and III, are the primary source and main targets of ROS.<sup>11</sup> In the present study, TEM analysis results revealed that the mitochondria in HG-cultured hDPCs had cristae disarrangement and ablation, which provided structural evidence for mtROS attack on the ETC. Based on this finding, we inferred that the MMP depolarization and reduced ATP synthesis may be attributable to the damaged structure of the ETC caused by mtROS overproduction.

Excessive production of mtROS promotes oxidative damage to mitochondrial biogenesis, which is essential for maintaining homeostasis of the mitochondrial mass and function.<sup>30</sup> In the present study, gene expression of major biogenesis-related markers was evaluated including *PGC-1 $\alpha$* , *TFAM*, *Nrf1*, and *Nrf2*. *PGC-1 $\alpha$*  is the master regulator of biogenesis. It activates its downstream targets *Nrf1* and *Nrf2*, leading to the expression of several mitochondrial genes, including proteins that are required for mitochondrial DNA transcription and replication, namely *TFAM*.<sup>31</sup> In this study, mRNA expression of *PGC-1 $\alpha$* , *TFAM*, *Nrf1*, *Nrf2* was upregulated under high-glucose conditions, suggesting compromised mitochondrial biogenesis. Similar to our findings, some studies have explored the effect of hyperglycemia on the mitochondrial biogenesis pathway, wherein mRNA expression of *PGC-1 $\alpha$*  had decreased in Schwann cells<sup>32</sup> and *TFAM* had decreased in keratinocytes.<sup>33</sup> These data may help provide potential targets to increase mitochondrial biogenesis and improve mitochondrial function in impaired diabetic pulp healing.

Besides, oxidative attack by mtROS can lead to the imbalance in mitochondrial dynamics including fusion and fission, which are critical in shaping the mitochondrial network and quality control.<sup>34</sup> The key components of the machinery mediating mitochondrial fusion belong to the dynamin superfamily, including *OPA1*, *Mfn1*, and *Mfn2*.<sup>35</sup> In this study, high glucose downregulated the mRNA expression of *OPA1*, whereas no significant difference was observed in *Mfn1* and *Mfn2* between the control and HG group. The *Mfn1* and *Mfn2* are located on the mitochondrial outer membrane and are required for outer membrane fusion; and the inner membrane fusion is mediated by *OPA1*.<sup>35</sup> Thus, it could be inferred that HG treatment affected the inner membrane fusion, not the outer membrane fusion in hDPCs. The compromised inner membrane fusion may be one of explanations for the damaged ultra-structure of mitochondrial cristae. The central mediator of mitochondrial fission is *Drp1*. This protein is recruited from

a cytosolic pool onto mitochondrial surface when orchestrating the mitochondrial fission.<sup>35</sup> Fis1 is located in the outer membrane to recruit Drp1 in yeast, whereas the role of Fis1 in Drp1 recruitment and mitochondrial fission in mammals remains to be clarified.<sup>36</sup> Our findings showed that mRNA expression of Drp1 and Fis1 was upregulated in the high-glucose environment, indicating increased mitochondrial fission. However, the role of Fis1 in this phenomenon needs to be further elucidated.

The present study has a limitation. The in vitro high-glucose condition does not fully reflect the conditions of the dental pulp tissue in DM. In the present study, supplementation of MT effectively improved the proliferation, migration, and odontoblastic differentiation of hDPCs and attenuated their apoptosis in vitro. A recent study suggested that MT treatment could counteract doxorubicin-induced osteoporosis in zebrafish.<sup>37</sup> Another report revealed that administration of MT could improve coronary endothelial function and small conductance calcium-activated potassium channel activity after cardioplegic hypoxia/reoxygenation.<sup>38</sup> Therefore, there is a necessity for in vivo experiments to further investigate the potential therapeutic effect of MT on impaired diabetic pulp healing.

In conclusion, this study demonstrated that high glucose could trigger mitochondrial damage by augmenting mtROS generation in hDPCs, involving a reduced density of bioactive mitochondria, damage to the mitochondrial ultrastructure, depolarization of MMP, and decline in ATP synthesis, all of

which contribute to inhibited proliferation, migration, and odontoblastic differentiation, and enhanced apoptosis. Suppression of mtROS production as well as restoration of mitochondrial dysfunction may represent therapeutic targets for impaired pulp healing in individuals with DM.

## Declaration of competing interest

The authors have no conflicts of interest relevant to this article.

## Acknowledgments

This work was supported by the National Natural Science Foundation of China [grant numbers 82170945, 81870760].

## Appendix B. Supplementary data

Supplementary data to this article can be found online at <https://doi.org/10.1016/j.jds.2023.04.008>.

## Appendix

**Appendix Table 1** Primers used for quantitative real-time polymerase chain reaction analysis.

Genes	Accession No.	Primers (5' - 3') (F: forward; R: reverse)
PGC-1 $\alpha$	NM_013261.5	F: TCTGAGTCTGTATGGAGTGACCA R: GGCAATCCGTCTTCATCCAC
TFAM	NM_003201.3	F: CTGCTTGGAAAACCAAAAAGACC R: TCTTCAGCTTTCTGCGGT
Nrf1	NM_001293163.2	F: ACAGGGAGGTGAGATGACCA R: GATCTGCCATAAAGAGGCCATT
Nrf2	NM_001313904.1	F: TAGATGAAGAGACAGGTTGCC R: CCGTCTAAATCAACAGGGGCT
OPA1	NM_130837.3	F: TTAGAAAGGGTCTGCTTGGTGA R: TGACACCTTGCCTTCTGTT
Mfn1	NM_033540.3	F: GCCACATGTAGTTATGTTCT R: AGGCTTAATGCCCTAGTGT
Mfn2	NM_014874.4	F: GGAAGGTGAAGTCAGGACTGGT R: GAAGAGCAGGGACATTGCGTT
Drp1	NM_001330380.1	F: TGACCCCTGCTACATGGAAAAAC R: CAGGCACCTGGTCATTCCCT
Fis1	NM_016068.3	F: CCAAGAGCACGCAGTTGAG R: ACGTAATCCGCTGTTCCCTC
$\beta$ -actin	NM_001101.5	F: CATGTACGTTGCTATCCAGGC R: CTCCTTAATGTCAAGCACGAT

PGC-1 $\alpha$ , peroxisome proliferator-activated receptor-gamma co-activator-1alpha; TFAM, mitochondrial transcription factor A; Nrf1, nuclear respiratory factor 1; Nrf2, nuclear respiratory factor 2; OPA1, optic atrophy 1; Mfn1, mitofusin 1; Mfn2, mitofusin 2; Drp1, dynamin-related protein 1; Fis1, mitochondrial fission 1.

## References

1. Cole JB, Florez JC. Genetics of diabetes mellitus and diabetes complications. *Nat Rev Nephrol* 2020;16:377–90.
2. Demir S, Nawroth PP, Herzig S, Ekim Ustunel B. Emerging targets in type 2 diabetes and diabetic complications. *Adv Sci* 2021;8:e2100275.
3. Lee YH, Kim HS, Kim JS, et al. C-myb regulates autophagy for pulp vitality in glucose oxidative stress. *J Dent Res* 2016;95: 430–8.
4. Moraru AI, GheorghiTa LM, Dascalu IT, et al. Histological and immunohistochemical study on the dental pulp of patients with diabetes mellitus. *Roman J Morphol Embryol = Rev roumain morphol embryol* 2017;58:493–9.
5. Garber SE, Shabahang S, Escher AP, Torabinejad M. The effect of hyperglycemia on pulpal healing in rats. *J Endod* 2009;35: 60–2.
6. Yan L, Sun S, Qu L. Insulin-like growth factor-1 promotes the proliferation and odontoblastic differentiation of human dental pulp cells under high glucose conditions. *Int J Mol Med* 2017;40:1253–60.
7. Li X, Xu W, Lin X, Wu J, Wu B. Effect of LncRNA-MALAT1 on mineralization of dental pulp cells in a high-glucose microenvironment. *Front Cell Dev Biol* 2022;10:921364.
8. Brownlee M. The pathobiology of diabetic complications: a unifying mechanism. *Diabetes* 2005;54:1615–25.
9. Giacco F, Brownlee M. Oxidative stress and diabetic complications. *Circ Res* 2010;107:1058–70.
10. Sharma K. Mitochondrial hormesis and diabetic complications. *Diabetes* 2015;64:663–72.
11. Schofield JH, Schafer ZT. Mitochondrial reactive oxygen species and mitophagy: a complex and nuanced relationship. *Antioxidants Redox Signal* 2021;34:517–30.
12. Forrester SJ, Kikuchi DS, Hernandes MS, Xu Q, Griendl KK. Reactive oxygen species in metabolic and inflammatory signaling. *Circ Res* 2018;122:877–902.
13. Zandalinas SI, Mittler R. ROS-induced ROS release in plant and animal cells. *Free Radic Biol Med* 2018;122:21–7.
14. Yu L, Liang Q, Zhang W, et al. HSP22 suppresses diabetes-induced endothelial injury by inhibiting mitochondrial reactive oxygen species formation. *Redox Biol* 2019;21:101095.
15. Sun X, Mao Y, Dai P, et al. Mitochondrial dysfunction is involved in the aggravation of periodontitis by diabetes. *J Clin Periodontol* 2017;44:463–71.
16. Hu XF, Wang L, Lu YZ, et al. Adiponectin improves the osteointegration of titanium implant under diabetic conditions by reversing mitochondrial dysfunction via the AMPK pathway in vivo and in vitro. *Acta Biomater* 2017;61:233–48.
17. Feng YF, Wang L, Zhang Y, et al. Effect of reactive oxygen species overproduction on osteogenesis of porous titanium implant in the present of diabetes mellitus. *Biomaterials* 2013; 34:2234–43.
18. Demyanenko IA, Popova EN, Zakharova VV, et al. Mitochondria-targeted antioxidant SkQ1 improves impaired dermal wound healing in old mice. *Aging* 2015;7:475–85.
19. Fayazipour D, Deckert J, Akbari G, Soltani E, Chmielowska-Bak J. Mitochondria specific antioxidant, MitoTEMPO, modulates Cd uptake and oxidative response of soybean seedlings. *Antioxidants* 2022;11:2099.
20. Ma T, Huang X, Zheng H, et al. SFRP2 Improves Mitochondrial dynamics and mitochondrial biogenesis, oxidative stress, and apoptosis in diabetic cardiomyopathy. *Oxid Med Cell Longev* 2021;2021:9265016.
21. Brownlee M. Biochemistry and molecular cell biology of diabetic complications. *Nature* 2001;414:813–20.
22. Forbes JM, Thorburn DR. Mitochondrial dysfunction in diabetic kidney disease. *Nat Rev Nephrol* 2018;14:291–312.
23. Huang S, Zheng B, Jin X, et al. Blockade of cyclophilin D attenuates oxidative stress-induced cell death in human dental pulp cells. *Oxid Med Cell Longev* 2019;2019:1729013.
24. Guo X, Chen J. The protective effects of saxagliptin against lipopolysaccharide (LPS)-induced inflammation and damage in human dental pulp cells. *Artif Cells Nanomed Biotechnol* 2019; 47:1288–94.
25. Wu D, Yan L, Zheng C, et al. Akt-GSK3beta-mPTP pathway regulates the mitochondrial dysfunction contributing to odontoblasts apoptosis induced by glucose oxidative stress. *Cell Death Dis* 2022;8:168.
26. Uzunoglu-Ozyurek E, Onal G, Dokmeci S. Odonto/Osteogenic differentiation of dental pulp stem cells of type 1 diabetic patients with mineral trioxide aggregate/1alpha,25-dihydroxyvitamin D3 combination. *J Endod* 2022;48:516–26.
27. Kichenbrand C, Grossin L, Menu P, Moby V. Behaviour of human dental pulp stem cell in high glucose condition: impact on proliferation and osteogenic differentiation. *Arch Oral Biol* 2020;118:104859.
28. Bhandi S, Alkahtani A, Mashyakhy M, et al. Study of optimal conditions for growth and osteogenic differentiation of dental pulp stem cells based on glucose and serum content. *Saudi J Biol Sci* 2021;28:6359–64.
29. Cano Sanchez M, Lancel S, Boulanger E, Neviere R. Targeting oxidative stress and mitochondrial dysfunction in the treatment of impaired wound healing: a systematic review. *Antioxidants* 2018;7:98.
30. Popov LD. Mitochondrial biogenesis: an update. *J Cell Mol Med* 2020;24:4892–9.
31. Cardanho-Ramos C, Morais VA. Mitochondrial biogenesis in neurons: how and where. *Int J Mol Sci* 2021;22:13059.
32. Zhang Q, Song W, Zhao B, et al. Quercetin attenuates diabetic peripheral neuropathy by correcting mitochondrial abnormality via activation of AMPK/PGC-1alpha pathway in vivo and in vitro. *Front Neurosci* 2021;15:636172.
33. Rizwan H, Pal S, Sabnam S, Pal A. High glucose augments ROS generation regulates mitochondrial dysfunction and apoptosis via stress signalling cascades in keratinocytes. *Life Sci* 2020; 241:117148.
34. Giacomello M, Pyakurel A, Glytsou C, Scorrano L. The cell biology of mitochondrial membrane dynamics. *Nat Rev Mol Cell Biol* 2020;21:204–24.
35. Chan DC. Mitochondrial dynamics and its involvement in disease. *Annu Rev Pathol* 2020;15:235–59.
36. Bui HT, Shaw JM. Dynamin assembly strategies and adaptor proteins in mitochondrial fission. *Curr Biol* 2013;23:R891–9.
37. Poudel S, Martins G, Cancela ML, Gavaia PJ. Regular supplementation with antioxidants rescues doxorubicin-induced bone deformities and mineralization delay in zebrafish. *Nutrients* 2022;14:4959.
38. Song Y, Xing H, He Y, et al. Inhibition of mitochondrial reactive oxygen species improves coronary endothelial function after cardioplegic hypoxia/reoxygenation. *J Thorac Cardiovasc Surg* 2022;164:e207–26.